YMTHE, Volume *26*

Supplemental Information

Nanoparticles Based on Poly (β-Amino Ester) and HPV16-Targeting CRISPR/shRNA as Potential Drugs for HPV16-Related Cervical Malignancy

Da Zhu, Hui Shen, Songwei Tan, Zheng Hu, Liming Wang, Lan Yu, Xun Tian, Wencheng Ding, Ci Ren, Chun Gao, Jing Cheng, Ming Deng, Rong Liu, Junbo Hu, Ling Xi, Peng Wu, Zhiping Zhang, Ding Ma, and Hui Wang

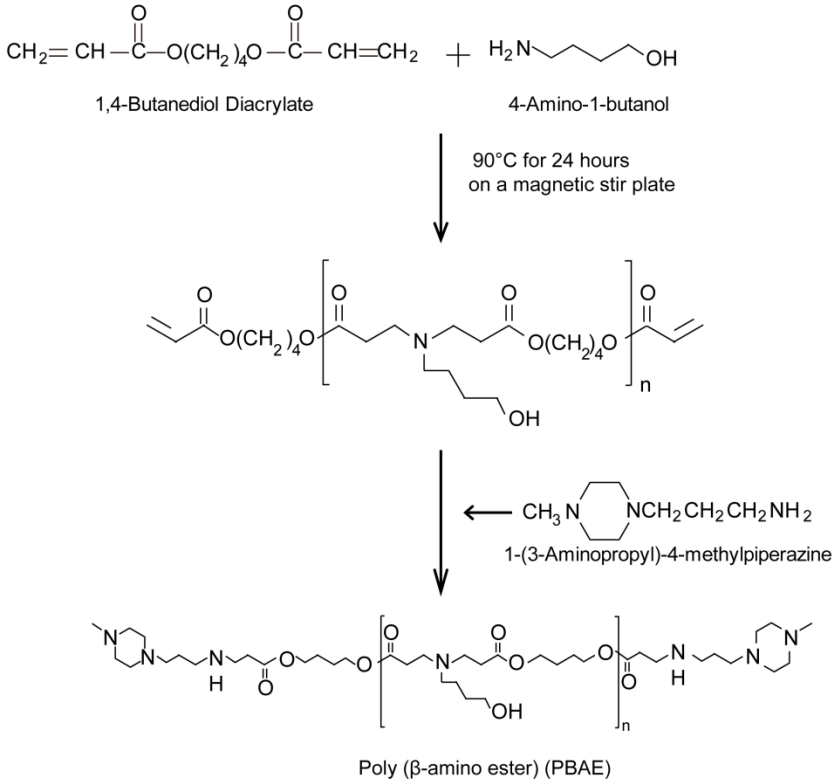

Figure S1. Synthesis of PBAE. 1,4-Butanediol diacrylate was mixed with 4-amino-1-butanol and stirred on a magnetic stir plate at 90°C for 24 hours. 1-(3-Aminopropyl)-4-methylpiperazine was added to the mixture and stirred to form the PBAE nanomaterials.

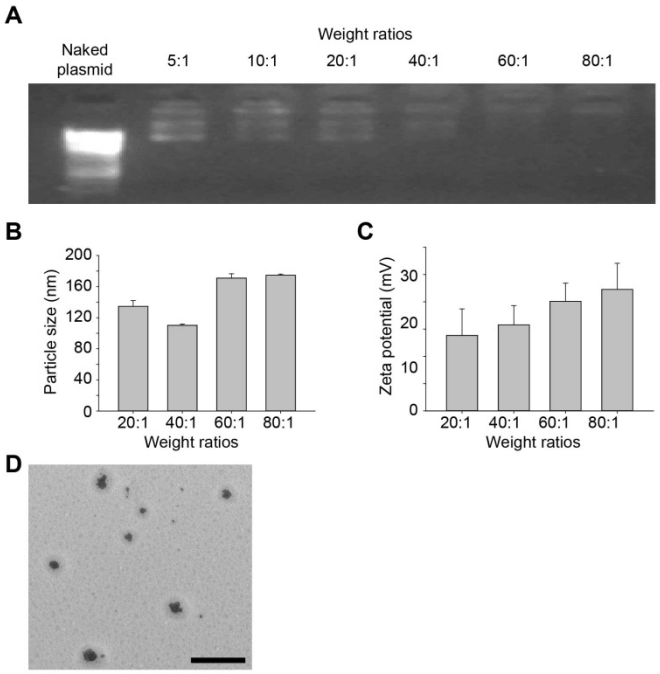

Figure S2. Physicochemical and morphological characterization of NPs. (A) Agarose gel electrophoresis of NPs containing a GFP plasmid with different weight ratios (PBAE:GFP). **(B)** Particle sizes and **(C)** zeta potentials of NPs with different weight ratios (PBAE:GFP) measured by dynamic light scattering. The data represent the mean ± SD (n = 3 per group). The data represent the mean ± SD (n = 3 per group). **(D)** TEM imaging of PBAE/GFP NPs (weight ratio 60:1). Scale bar, 500nm.

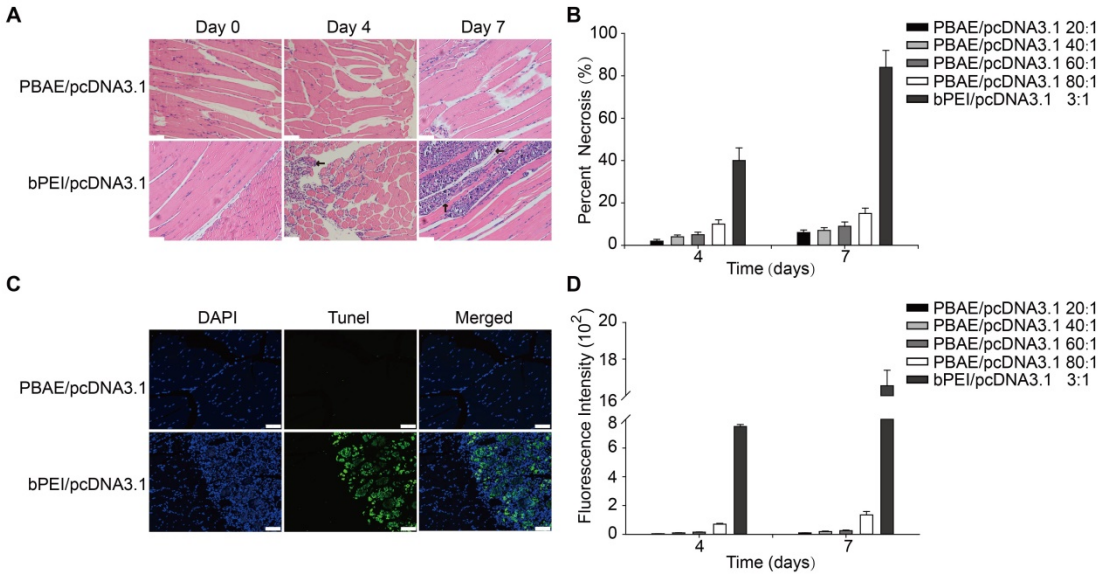

Figure S3. Toxicity of NPs in mouse thigh muscles. (A) Representative images of H&E staining and **(B)** necrosis percentage of mouse thigh muscles injected with NPs consisting of PBAE/pcDNA3.1 (weight ratio 60:1) or bPEI/pcDNA3.1 (weight ratio 3:1). Arrows indicate the necrotic areas. Scale bars, 40 μm. The data represent the mean ± SD (n = 3). **(C)** Representative images of TUNEL staining and **(D)** TUNEL fluorescence intensity of mouse thigh muscles injected with NPs consisting of PBAE/pcDNA3.1 or bPEI/pcDNA3.1. Green fluorescence indicates TUNEL staining. Scale bars, 40 μm. The data represent the mean ± SD (n = 3). Mouse thigh muscles were injected with our NPs containing 10 μg of DNA once a day for three days and then harvested, and the toxicity was evaluated by H&E staining and TUNEL staining on the 4th day and 7th day after the initial injection. The NPs were compared with bPEI/pcDNA3.1 (weight ratio 3:1) complexes.

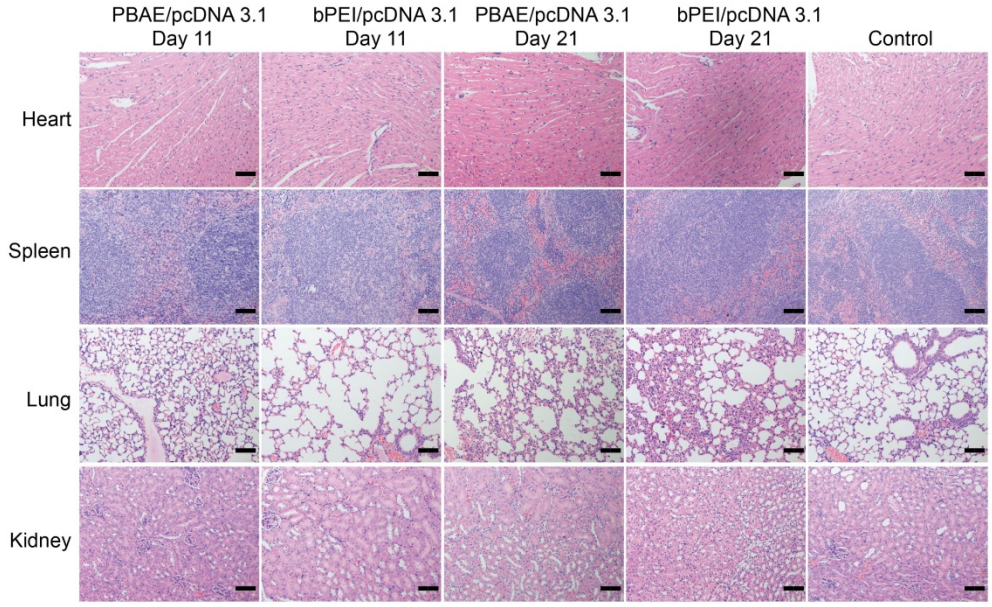

Figure S4. Toxicity of NPs in the organs of mice whose vaginas were pipetted with NPs. Representative images of H&E staining of the hearts, spleens, lungs and kidneys of mice whose vaginas were pipetted with NPs. The NPs consisted of PBAE/pcDNA3.1 (weight ratio 60:1) or bPEI/pcDNA3.1 (weight ratio 3:1). The mouse vaginas were pipetted with NPs carrying 10 μg of plasmid once per day for 20 days, and the organs were harvested on the 11th and 21st days after the initial pipetting. Scale bars, 40 μm.

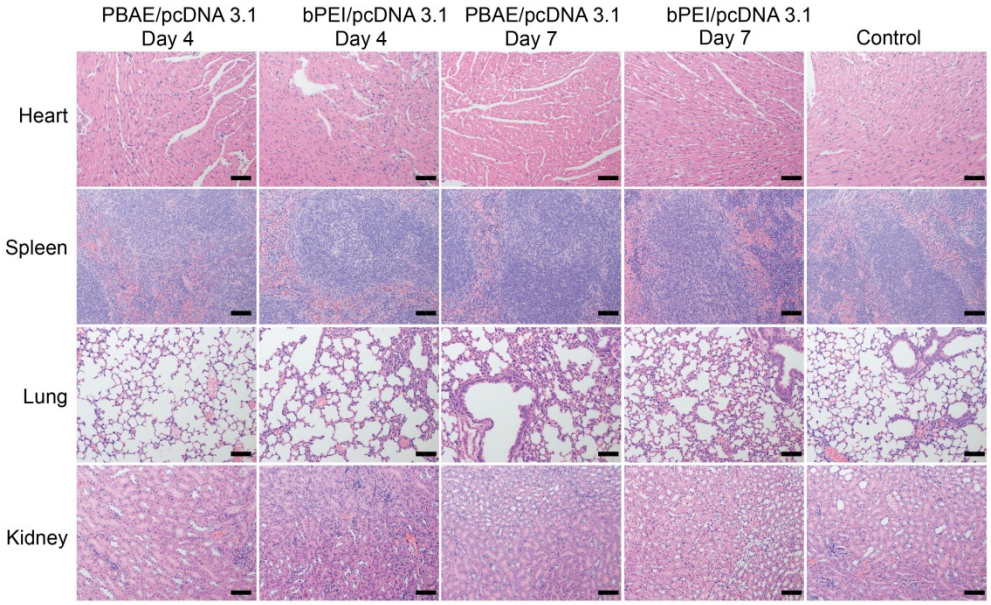

Figure S5. Toxicity of NPs in the organs of mice whose thigh muscles were injected with NPs. Representative images of H&E staining of the hearts, spleens, lungs and kidneys of mice whose thigh muscles were injected with NPs. The NPs consisted of PBAE/pcDNA3.1 (weight ratio 60:1) or bPEI/pcDNA3.1 (weight ratio 3:1). The mouse thigh muscles were injected with NPs carrying 100 μg of plasmid once per day for three days and the organs harvested on the 4th and 7th days after the initial injection. Scale bars, 40 μm.

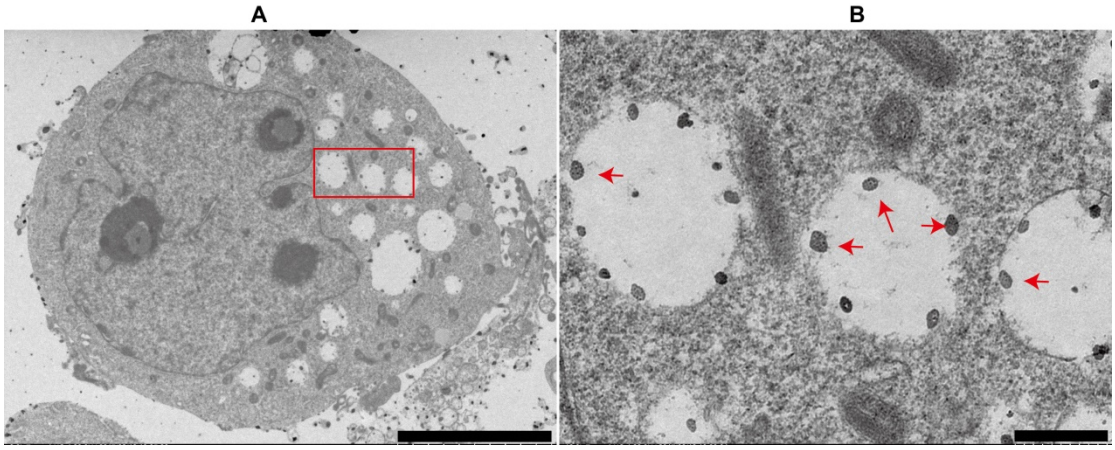

Figure S6. Transmission electron microscopy (TEM) imaging of 293 cells transfected with PBAE/GFP NPs. NPs were in the vesicles of the cytoplasm, indicating the endocytosis. Figure (B) (Scale bar, 500 nm) was enlarged red box in figure (A) (Scale bar, 5 μm). Arrows showed NPs. Cells were fixed after 72 hours transfection.

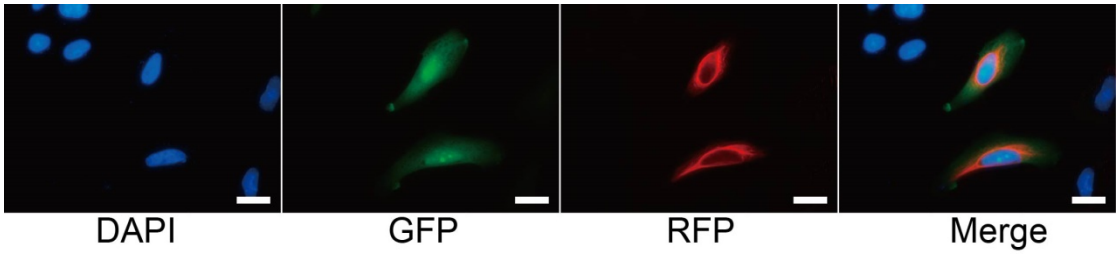

Figure S7. GFP plasmids were released from the PBAE/GFP NPs. After PBAE/GFP NPs were taken up by SiHa cells, GFP plasmids were released into the cytoplasm and expressed GFP proteins (green). Anti-GFP immunofluorescence (RFP, red) staining further confirmed the cytoplasm location of GFP proteins. Fixed cells were stained with DAPI for nuclei (blue) and rabbit anti-GFP (RFP, red) for GFP proteins. Scale bars, 20μm.

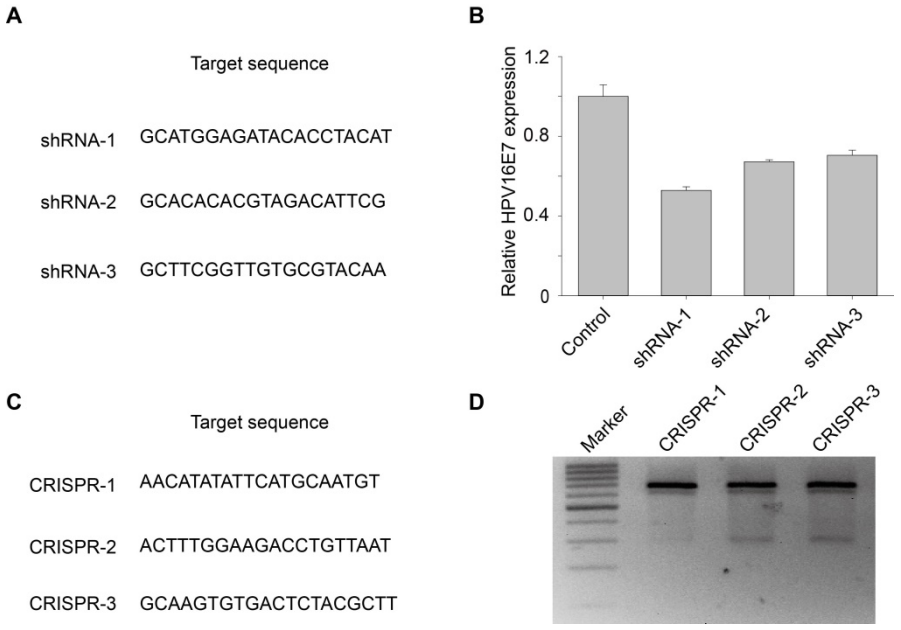

Figure S8. Choose of HPV16E7 targeting shRNA and CRISPR. (A) sequences of HPV16E7 targeting shRNAs. **(B)** The effect of silencing HPV 16 E7 of the three shRNAs on SiHa cells. The expression of HPV16 E7 was measured by RT-PCR. (C) Targed sequences of HPV16E7 targeting CRISPR. **(D)** T7E1 assay of the three CRISPR.

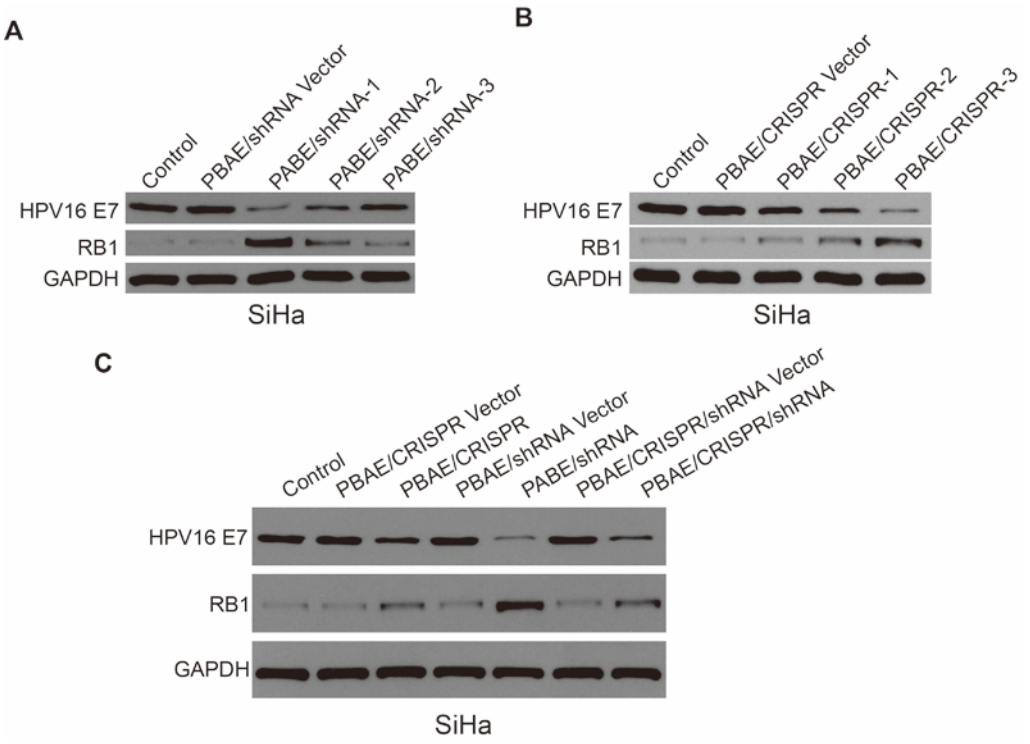

Figure S9. HPV16 *E7*-targeting ability of NPs in SiHa cells. The HPV16 *E7* and *RB1* protein expression levels in SiHa cells 72 hours after (**A**) PBAE/shRNAs NPs and (**B**) PBAE/CRISPRs NPs treatment. ShRNA-1 and CRISPR-3 were selected for further experiments. (**C**) The HPV16 *E7* and *RB1* protein expression levels in SiHa cells 72 hours after PBAE/shRNA/CRISPR combined NPs treatment. Protein expression levels were determined by western blotting analysis (PBAE/plasmid, weight ratio 60:1, 1 ng/μl plasmid).

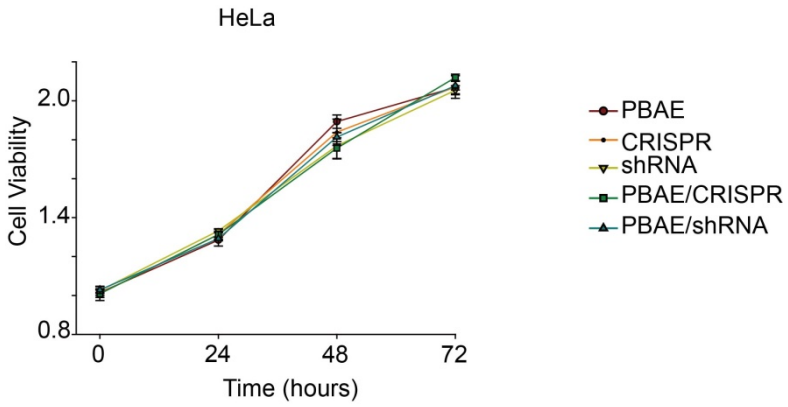

Figure S10. HPV16 *E7*-targeting ability of NPs in HPV16-negative (HPV18 positive) cervical cell line. The cell viabilities of HeLa cells were determined 0, 24, 48 and 72 hours after HPV16 *E7*-targeting NP treatment by CCK-8 assay (PBAE/CRISPR and PBAE/shRNA, weight ratio 60:1, 1 ng/μl plasmid). The data represent the mean ± SD (n =3).